Nanoscale

PAPER

View Article Online
View Journal | View Issue

Cite this: *Nanoscale*, 2015, **7**, 10178

Ultra-stretchable conductors based on buckled super-aligned carbon nanotube films†

Yang Yu,[a,b] Shu Luo,[a,b] Li Sun,[a] Yang Wu,[a] Kaili Jiang,[a,c] Qunqing Li,[a,c] Jiaping Wang*[a,c] and Shoushan Fan[a,b]

Received 3rd March 2015,
Accepted 1st May 2015

DOI: 10.1039/c5nr01383f

www.rsc.org/nanoscale

Ultra-stretchable conductors are fabricated by coating super-aligned carbon nanotube (SACNT) films on pre-strained polydimethylsiloxane (PDMS) substrates and forming buckled SACNT structures on PDMS after release of the pre-strain. The parallel SACNT/PDMS conductors demonstrate excellent stability with normalized resistance changes of only 4.1% under an applied strain as high as 200%. The SACNT/PDMS conductors prepared with cross-stacked SACNT films show even lower resistance variation. The parallel SACNT/PDMS conductors exhibit high durability with a resistance increase of less than 5% after 10 000 cycles at 150% strain. *In situ* microscopic observations demonstrate that the buckled SACNT structures are straightened during the stretching process with reversible morphology evolution and thus the continuous SACNT conductive network can be protected from fracture. Due to the excellent electrical and mechanical properties of SACNT films and the formation of the buckled structure, SACNT/PDMS films exhibit high stretchability and durability, possessing great potential for use as ultra-stretchable conductors for wearable electronics, sensors, and energy storage devices.

1. Introduction

With the increasing development of stretchable electronics, conductors that can remain electrically conductive under large strains become quite critical for many new applications such as stretchable energy devices and human-motion sensors.[1–3] Many stretchable material structures such as wavy metal films, carbon nanotube/polymer composite films, and graphene/polymer composite films have been developed that demonstrate excellent conductivity and mechanical robustness by the design of wave-like or net-shaped structures.[4–9] Carbon nanotubes (CNT) are considered as among the promising materials for stretchable conductors due to their large aspect ratio, excellent electrical conductivity, high thermal stability, and mechanical robustness.[10–12] Many stretchable conductors based on CNT/polymer composites have been reported in the literature.[13–16] In these composite structures, CNTs form a continuous and conductive network, and the polymer matrix offers excellent stretchability and protects the CNT network from fracture. Typical CNT/polymer stretchable structures reported so far include rubberlike conductive composites with uniform dispersion of single-walled CNTs (SWCNTs) in a polymer matrix,[13] transparent and conductive films with randomly distributed CNTs sprayed on a stretchable polymer film,[14] and buckled electrodes fabricated by laminating a randomly oriented SWCNT film on a pre-strained polydimethylsiloxane (PDMS) substrate.[15,16] Although high conductivity and stretchability were demonstrated in these structures, there still exist several limitations for practical applications, such as a complicated fabrication process, deteriorated conductivity under large applied strain, and poor durability. In these composites, CNTs were randomly oriented with weak bonding among tubes and the CNT junctions may fracture under large applied strains and cause resistance increase. Repeated tensile loading may further break the CNT junctions and result in more resistance variation. Therefore, the randomly oriented CNT films may not be the best choice for stretchable conductors.

Super-aligned CNTs (SACNTs) have attracted much attention over the years.[17,18] Ultrathin and continuous SACNT films can be easily drawn from SACNT arrays by an end-to-end joining mechanism, which is cost-effective and environmentally benign. The alignment of CNTs in the SACNT film is parallel to the drawing direction. The SACNT films are freestanding, lightweight, and possess excellent electrical and mechanical properties along their axial direction.[19,20] By cross-stacking SACNT layers, SACNT films with isotropic electrical conductivity can be obtained. The thickness of the SACNT

[a]*Department of Physics and Tsinghua-Foxconn Nanotechnology Research Center, Tsinghua University, Beijing 100084, China. E-mail: jpwang@tsinghua.edu.cn*
[b]*School of Materials Science and Engineering, Tsinghua University, Beijing 100084, China*
[c]*Collaborative Innovation Center of Quantum Matter, Beijing 100084, China*
†Electronic supplementary information (ESI) available. See DOI: 10.1039/c5nr01383f

film depends on the number of CNT layers. SACNT films have been widely used in loudspeakers,[21] touch screens,[22] electrodes for lithium ion batteries,[23–25] current collectors,[26,27] and so on.

In this work, high performance SACNT/PDMS stretchable conductors were fabricated by coating parallel or cross-stacked SACNT films on a flexible and pre-strained PDMS substrate. Buckled SACNT structures were formed on the PDMS substrate after release of the pre-strain. *In situ* microscopic observation demonstrated that the buckled SACNT structures were straightened during the stretching process with reversible morphology evolution and thus the SACNT conductive network could be protected from fracture. The SACNT/PDMS conductors remained highly conductive under an applied strain as high as 200% and withstood 10 000 stretching-releasing cycles at 150% strain with a resistance change less than 5%. The excellent stretchability and durability of the SACNT/PDMS conductive films are of great advantages over other carbon-based stretchable conductors reported in the literature.[13–15]

2. Results and discussion

2.1. Formation and resistance changes of the buckled SACNT/PDMS films

The fabrication processes of the buckled SACNT/PDMS conductors are schematically shown in Fig. 1a. Firstly, a PDMS substrate with a length of L is pre-strained to a length of $L + \Delta L$. Secondly, a continuous SACNT film is directly drawn from SACNT arrays on a Si wafer (Fig. 1b) and various layers of the SACNT films are then stacked onto the pre-strained PDMS substrate. Fig. 1c shows the scanning electron microscopy (SEM) image of an SACNT film, where parallel SACNT bundles can be clearly observed. After the PDMS substrate is released to its original length L, buckled SACNT structures are formed on the PDMS substrate (Fig. 1d). The inset of Fig. 1a shows the photograph of a highly flexible SACNT/PDMS composite film with the buckled structure.

Buckled SACNT/PDMS conductors with various layers of SACNT films were fabricated. The PDMS substrates were first stretched to a pre-strain of 40%. 2, 6, and 10 layers of SACNT films were then stacked onto the pre-strained PDMS substrates. After release of the pre-strain, buckled SACNT/PDMS composite films were obtained. Tensile strain was applied using an Instron 5848 microtester and the resistance changes of the SACNT/PDMS films under applied strains up to 60% were monitored using a Keithley 2400 Source Meter at the same time. The sheet resistance of a single layer of the SACNT film along the drawing direction is about 1000 Ω sq^{-1}.[22] As the number of SACNT layers increased from 2 to 6 and 10, the initial resistances of the SACNT/PDMS composites decreased from 684 to 430 and 186 Ω (Fig. S1†). The normalized resistance changes ($\Delta R/R_0$) of these SACNT/PDMS films as a function of the applied strain are plotted in Fig. 2. The resistances of the SACNT/PDMS composites with 2 and 6 layers of SACNT films kept almost constant when the applied tensile strain was smaller than the value of the pre-strain at 40%. After the applied strain exceeded 40%, the normalized resistance changes ($\Delta R/R_0$) gradually increased to 19% and 23% at 50% strain for the composites with 2 and 6 layers of SACNT films. For the SACNT/PDMS composite with 10 layers of SACNT films, although it showed the lowest initial resistance, a sharp increase of resistance occurred when the applied strain exceeded the level of pre-strain at 40%. The normalized resistance changes ($\Delta R/R_0$) increased dramatically to 125% at 50% strain due to the detached SACNT conductive bundles especially the top layers that have poor interaction with the surface of the PDMS substrate, as shown in Fig. S2.† Comparing the SACNT/PDMS composites with different layers of SACNT films, the 6-layer SACNT/PDMS composites demon-

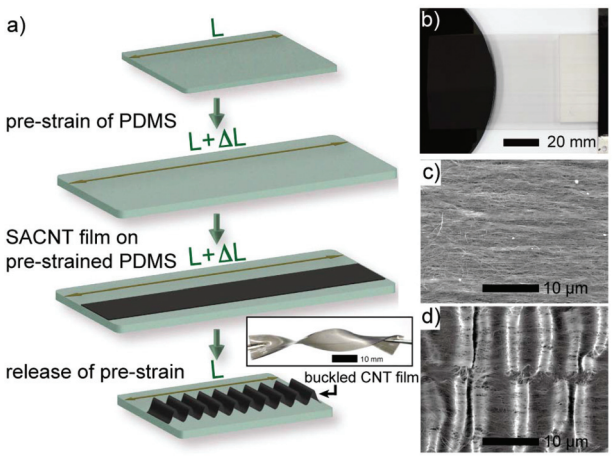

Fig. 1 (a) Schematic processes for fabricating a buckled SACNT/PDMS conductor and a photograph of a flexible sample; (b) photograph and (c) SEM image of an SACNT film; (d) SEM image of the buckled SACNT structures on a pre-strained PDMS substrate.

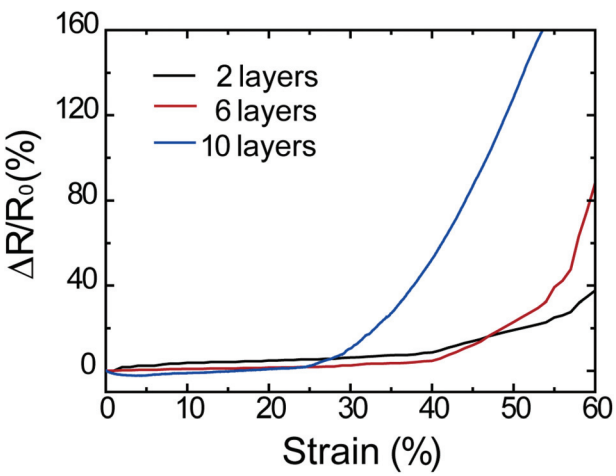

Fig. 2 Normalized resistance changes of the 40% pre-strained SACNT/PDMS conductors with 2, 6, and 10 layers of SACNT films as a function of the applied tensile strain.

strated both relatively low initial resistance and stability in enduring strains larger than the level of pre-strain, and thus are more suitable for use in real stretchable devices. The experiments and analyses below are all based on the SACNT/PDMS conductors with 6 layers of SACNT films.

SACNT/PDMS composites were also prepared with larger pre-strains of the PDMS substrate in order to obtain stretchable conductors that can maintain a constant conductivity under larger applied strains. Fig. 3a shows the relationship between the normalized resistance changes ($\Delta R/R_0$) and the applied strain in the SACNT/PDMS composites with no pre-strain, 40%, and 200% pre-strain. The SACNT/PDMS film with no pre-strain showed a sharp resistance increase during stretching with a normalized resistance increase of 632% at 40% strain, and such an increase in resistance is irreversible. As shown in Fig. 3b, after the SACNT/PDMS film with no pre-strain was loaded to 10% and 20% strains, upon unloading, the resistance could not recover to its original value, and the normalized resistance changes were around 20% and 80% respectively. In contrast, the SACNT/PDMS composites with pre-strains exhibited much more stable resistances when the applied strain was smaller than the level of pre-strain. For the SACNT/PDMS film with 40% pre-strain, the normalized resistance change was only 4% at 40% strain. The sample with 200% pre-strain could even withstand a strain as large as 200% with a normalized resistance change of only 4.1%. Moreover, the resistance changes of the SACNT/PDMS films with the pre-strain sample were fully reversible as long as the applied strain was smaller than the value of pre-strain. As shown in Fig. 3b, the resistance of the SACNT/PDMS films with 40% pre-strain almost recovered to its original value when the sample was loaded to 40% strain and then released to its original length. After the applied strain was increased to a value larger than the pre-strain, the resistance increased irreversibly. When the SACNT/PDMS film with 40% pre-strain was loaded with a 50% strain, the normalized resistance increase reached 20%. Such an increased resistance remained after the sample was unloaded, similar to the SACNT/PDMS film with no pre-strain.

2.2. *In situ* SEM observation of the buckled SACNT structures

A lab-designed tensile module was used to stretch the SACNT/PDMS composites within the SEM chamber to make *in situ* observation of the dynamic changes of the surface morphologies during the loading and releasing cycles. The morphologies of the SACNT/PDMS film with no pre-strain at its original stage and at 40% and 60% strains during the stretch process are shown in Fig. 4a. At the original stage, the SACNT films uniformly covered the PDMS substrate. At 40% strain, the SACNT bundles began to break and large gaps could be observed. Such gaps became wider when the strain was further increased to 60%. The fracture of SACNT films resulted in a sharp and irreversible increase in resistance, as shown in Fig. 3a and 3b.

In comparison, the formation and straightening of the wavy structures of the SACNT/PDMS film with 40% pre-strain during the release of the pre-strain and the following stretch process were revealed in sequence by *in situ* SEM observation (Fig. 4b). Firstly, the SACNT film was stacked on the PDMS substrate with 40% pre-strain (Fig. 4b(i)). The surface was smooth with straight and aligned SACNT bundles. Afterwards, the PDMS substrate was partially released to 20% strain and then to its original length. The SACNT film was compressed during the release of the PDMS substrate, meanwhile wavy and buckled structures of the SACNT films gradually formed on the PDMS substrate (Fig. 4b(ii)). Such buckled CNT structures were also reported in the literature and a buckling mechanism was proposed by considering the interaction among CNT bundles and the adhesion between CNTs and the substrate.[9] These buckled structures are out of the PDMS surface. Part of the CNT bundles adhered on the PDMS surface *via* the van der Waals force and the other part suspended in air, so the SACNT films detached from the PDMS substrate periodically, as shown in Fig. S3.† After the full release of the pre-strain,

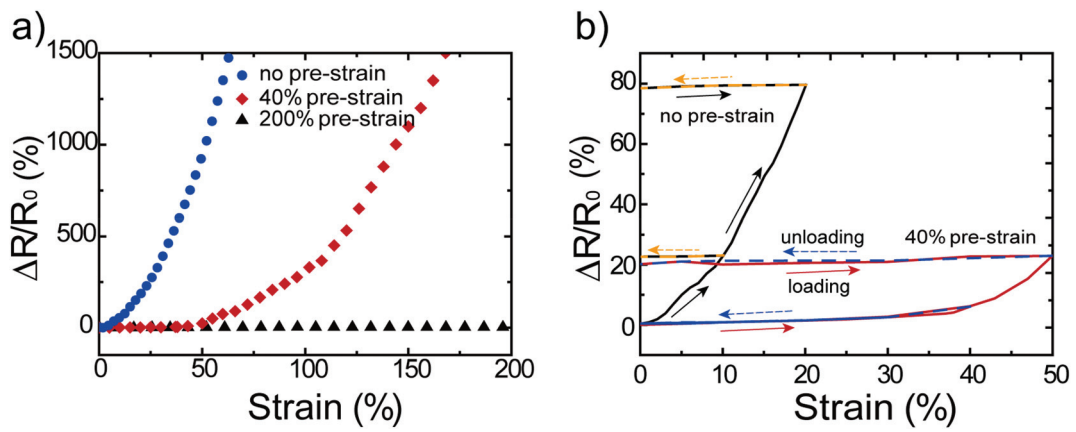

Fig. 3 Normalized resistance changes of the SACNT/PDMS films (a) with different pre-strains as a function of the applied tensile strain; (b) with no pre-strain and 40% pre-strain during loading–unloading cycles (loading: solid lines; unloading: dashed lines).

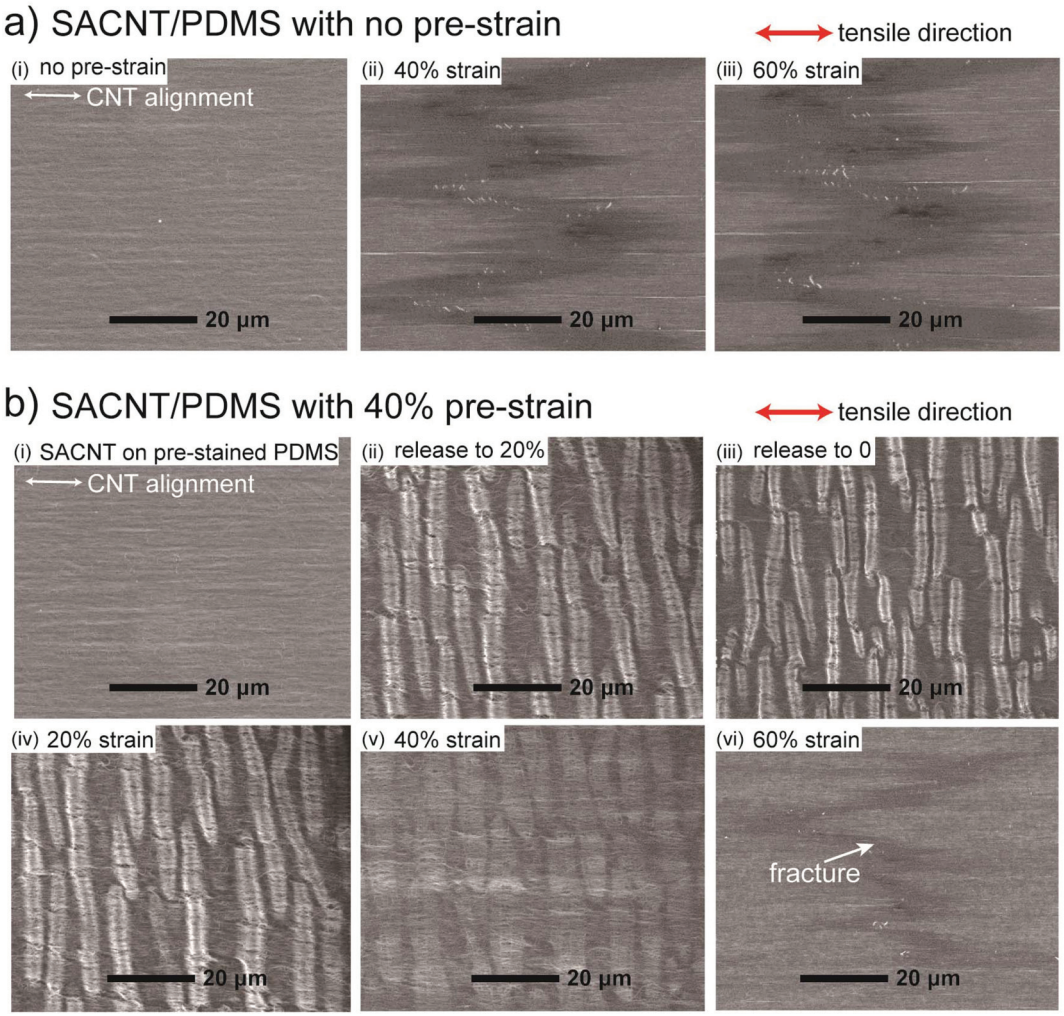

Fig. 4 *In situ* SEM images of (a) the SACNT/PDMS film with no pre-strain during stretching; (b) the SACNT/PDMS film with 40% pre-strain during the release of the pre-strain and further stretch.

strains of 20%, 40%, and 60% were applied to the buckled SACNT/PDMS composites along the direction of the pre-strain. During the stretch process, the wavy SACNT structures became gradually straightened. When the SACNT/PDMS composites were loaded with a strain equal to the value of pre-strain, *i.e.* 40%, the wavy structures were almost flattened (Fig. 4b(v)). The continuous and conductive SACNT network still remained intact without fracture of SACNTs. The integrity of the SACNT conductive network contributed to the steady resistance with only 4% normalized increase for the pre-strained SACNT/PDMS composite at applied strains smaller than the value of pre-strain (Fig. 3). In addition, as the buckling and straightening processes were reversible, the resistance of the SACNT/PDMS composite could be fully recovered to the original value upon unloading. As the applied strain was increased further to 60%, exceeding the pre-strain, the wavy structures became totally flattened and gaps perpendicular to the direction of the applied strain appeared, leading to the fracture of the SACNT films, as marked by the arrow in Fig. 4b(vi). The breakdown of the conductive SACNT network was responsible for the rapid and irreversible increase of the resistance at strains larger than the pre-strain in Fig. 3b (20% normalized resistance increase at 60% strain).

2.3. Cross-stacked SACNT/PDMS conductors

Cross-stacked SACNT films have isotropic electrical properties and have been widely used as conductors.[17] SACNT/PDMS composites were prepared by cross-stacking 6 layers of SACNT films on the pre-strained PDMS substrates, and their performances as stretchable conductors were compared with the SACNT/PDMS composites with parallel SACNT films. The initial resistance of the cross-stacked SACNT/PDMS composite was 497 Ω, which was slightly larger than that of the parallel SACNT/PDMS composite with the same layers of SACNT films (430 Ω). Fig. 5a shows the normalized resistance changes as a function of the applied strain for the 40% pre-strained SACNT/PDMS composites with parallel and cross-stacked SACNT films (denoted as "∥" and "⊥" CNT films). The normalized resistance

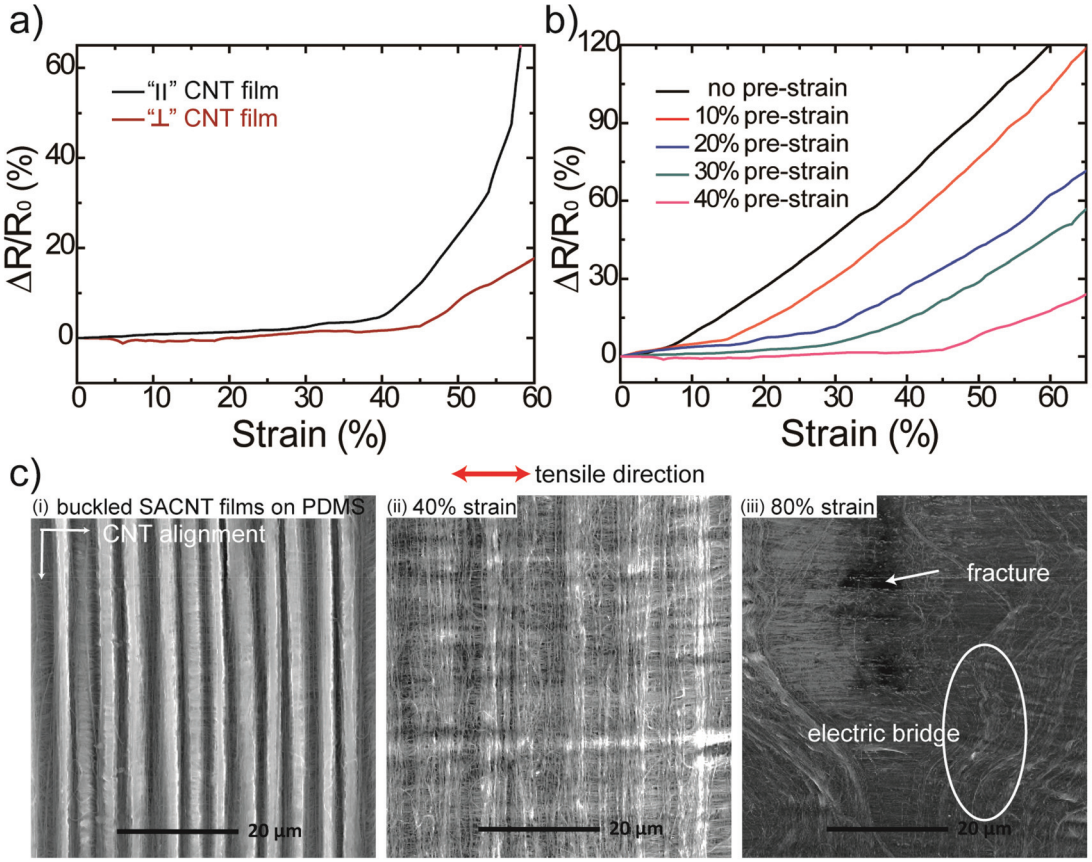

Fig. 5 (a) Normalized resistance changes of the 40% pre-strained parallel and cross-stacked SACNT/PDMS films as a function of the applied tensile strain; (b) resistance variations of the cross-stacked SACNT/PDMS films prepared with different pre-strains; (c) *in situ* SEM images of the wavy cross-stacked SACNT structures and the morphology evolution at applied strains of 40% and 80%.

increase was only 1.7% at 40% strain for the cross-stacked SACNT/PDMS composite, which presented a more constant resistance than the parallel SACNT/PDMS composite with 4% resistance change at the same strain. In particular, at strains larger than the pre-strain (40%), the normalized resistance increase of the cross-stacked SACNT/PDMS composite was much smaller than the parallel SACNT/PDMS composite. When the applied strain increased to 60%, the normalized resistance increase of the cross-stacked SACNT/PDMS composite was 18%, compared with a much larger increase of about 80% for the parallel SACNT/PDMS composite.

Fig. 5b shows the normalized resistance changes of the cross-stacked SACNT/PDMS films with different pre-strains from 0 to 40% as a function of the applied strain. Note that the cross-stacked SACNT/PDMS films were only pre-strained up to 40%. As the pre-strain increased to 60%, due to the lateral broadening of the PDMS substrate during the release of the pre-strain, the SACNT bundles aligned perpendicular to the tensile direction would suffer from tension stress. Some of these SACNT bundles fractured and resulted in large-area delamination of the SACNT film from the PDMS substrate and failure of the composite, as shown in Fig. S4.† Therefore, the value of pre-strain for the cross-stacked SACNT/PDMS films was limited to 40%. The trend of resistance variation with the applied strain was similar to that in the parallel SACNT/PDMS films. The resistance of the SACNT/PDMS film with no pre-strain increased rapidly as the strain increased. But for the SACNT/PDMS films with pre-strains, when the applied strain was smaller than the pre-strain, the resistance kept almost constant. When the applied strain was larger than the pre-strain, the resistance began to increase rapidly. *In situ* SEM images in Fig. 5c show the wavy cross-stacked SACNT structures on a 40% pre-strained substrate and the morphology evolution at applied strains of 40% and 80%. As the applied strain increased, the buckled SACNT structures were straightened gradually, similar to the parallel SACNT/PDMS films. When the applied strain was as high as 80%, exceeding the value of pre-strain at 40%, the cross-stacked SACNT films presented different features compared with the parallel SACNT films. Though the SACNT bundles along the direction of the tensile loading were fractured marked by the arrow in Fig. 5c (iii), the SACNT bundles aligned perpendicular to the tensile direction could still act as "electric bridges" to connect the gaps formed by the broken SACNT bundles along the tensile direction. Consequently, the conductive path could still be maintained in the SACNT/PDMS film, leading to the more

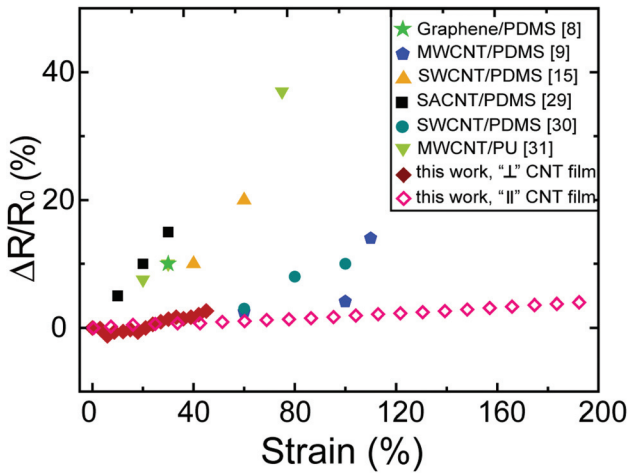

Fig. 6 Comparison of the stretchability and resistance stabilities between this work and other stretchable conductors based on carbon materials reported in the literature.

gentle resistance increase than that of the parallel SACNT/PDMS film as shown in Fig. 5a. The extreme low resistance variation of the cross-stacked SACNT/PDMS composite is beneficial for applications of resistance-sensitive devices such as stretchable conductors that are integrated with sensors.

The stretchable SACNT/PDMS conductors prepared in this work possess both excellent stretchability and resistance stability, compared with other carbon-based stretchable conductors reported in the literature.[8,9,13,15,28–31] As shown in Fig. 6, the SACNT/PDMS ultra-stretchable conductors exhibit the lowest resistance variation at the largest applied strain. The parallel SACNT/PDMS conductors can endure an applied strain as high as 200% with a normalized resistance increase of only 4.1%. The resistance of the cross-stacked SACNT/PDMS conductors can be maintained almost constant with a resistance change of only 1.7% at 40% strain. Such impressive performance could be attributed to the unique characteristics of the SACNT films. SACNT films with highly oriented SACNT bundles provide a conductive and robust network in the composite. Therefore the SACNT/PDMS films are highly flexible and conductive, which ensure the wavy structures to be fully recovered during the loading–unloading cycles. The continuous SACNT films remain intact at large strains below the value of the pre-strain that results in low resistance variation and high stretchability.

2.4. Durability of the SACNT/PDMS conductors

The durability of the parallel SACNT/PDMS conductor was characterized by performing cyclic tensile tests with 150% strain for 10 000 cycles and the resistance of the sample was monitored at each cycle. Fig. 7 shows the normalized resistance changes of the parallel SACNT/PDMS films with no pre-strain and with 200% pre-strain during the 10 000 cycles with 150% strain. The pre-strained SACNT/PDMS film demonstrated steady resistance during the cyclic tensile loading. Even after 10 000 cycles, the normalized resistance increase was still less than 5%. In contrast, the resistance of the SACNT/PDMS film with no pre-strain was about 45 times its original value after the first cycle, and such a large resistance remained during the following cycles. Fig. S5† shows the durability of a cross-stacked PDMS/SACNT film with 40% pre-strain for 10 000 cycles at 40% strain. The normalized resistance increase was about 7.5% after 10 000 cycles, which was larger than that of the parallel SACNT/PDMS films. In the cross-stacked PDMS/SACNT film, SACNT bundles aligned perpendicular to the tensile direction suffered from cyclic tensile stress during the unloading processes due to the lateral broadening of the PDMS substrate. Fracture of these SACNT bundles resulted in the resistance increase and thus affected the durability of the cross-stacked PDMS/SACNT film.

The morphologies of the parallel SACNT/PDMS films with no pre-strain and with 200% pre-strain were examined by SEM before and after the cyclic tensile testing. For the sample with no pre-strain, the SACNT bundles were broken and huge gaps formed under an applied strain of 40% (Fig. 8a), leading to a dramatic increase in resistance. Such gaps could not be recovered during the unloading process, therefore such a resistance increase was irreversible in the following cycles. However, for

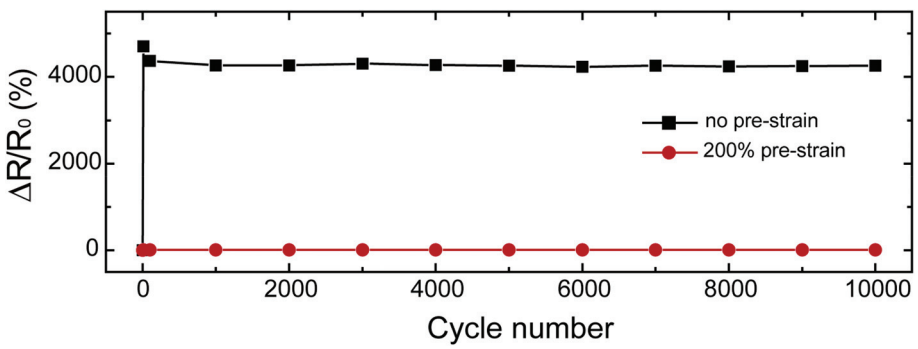

Fig. 7 Normalized resistance changes of the parallel SACNT/PDMS films with no pre-strain and 200% pre-strain during 10 000 cycles at 150% strain.

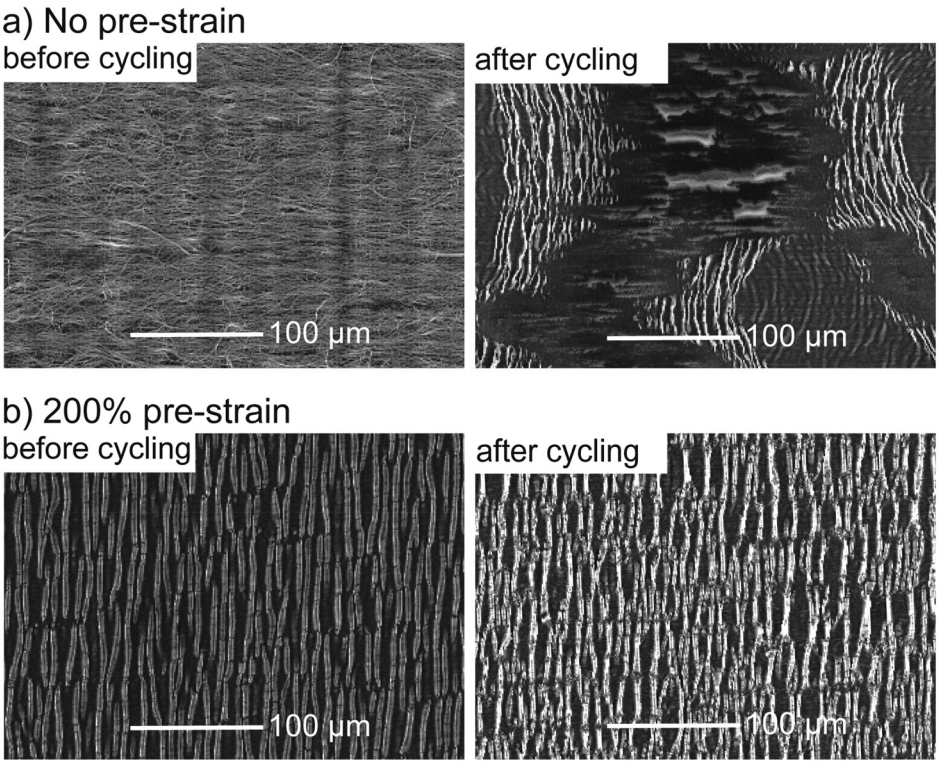

Fig. 8 SEM images of the SACNT/PDMS films (a) with no pre-strain and (b) with 200% pre-strain before and after 10 000 tensile cycles at 150% strain.

the pre-strained SACNT/PDMS films, the buckled SACNT structures could be straightened and formed repeatedly without fracture of the conductive SACNT network (Fig. 8b). No evident structural failures were present in the pre-strained sample after 10 000 tensile cycles except for very small gaps perpendicular to the tensile direction caused by the repeated loading–unloading processes. These results further demonstrate the strong interaction between the SACNT bundles and the PDMS substrate that can ensure the structural stability of the SACNT/PDMS films for 10 000 cycles. Due to the excellent mechanical performance and recovery capability of the SACNT films at strains below the pre-strain, the continuous SACNT conductive network could be well maintained. Thus ultra-high durability was achieved in the pre-strained SACNT/PDMS films with almost constant resistance during the long-term loading cycles. The high durability of the SACNT/PDMS films is of great value for use in stretchable devices.

Finally, in order to test the practical performance of the SACNT/PDMS stretchable conductor, a series circuit was constructed that connected an LED with the SACNT/PDMS film prepared with a pre-strain of 100% and a Keithley source meter with a stabilized output of 10 V. Fig. 9a shows a photograph of the illuminated LED without applying any strain. Afterwards, the SACNT/PDMS composite film was stretched to a 100% strain using a microtester, and the LED did not show any noticeable luminance fluctuation as shown in Fig. 9b,

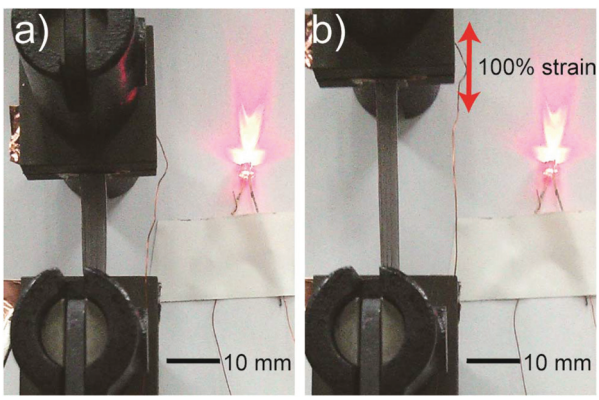

Fig. 9 (a) An illuminated LED in a circuit connected with a SACNT/PDMS conductor; (b) photograph of the LED under an applied strain of 100%.

revealing that the resistance change of the SACNT/PDMS conductor was ignorable during stretching. In order to improve the anti-scratch properties of the SACNT/PDMS conductors in various applications, a thin layer of PDMS was spin-coated on the buckled SACNT/PDMS films to prevent damage from exterior physical contacts. The initial resistance of the SACNT/PDMS films remained almost constant after the spin-coating process. The normalized resistance increase of the spin-coated

SACNT/PDMS composite during stretching was comparable to those without the spin-coating process. Combining the advantages of the facile fabrication and high stretchability and excellent durability, the SACNT/PDMS films demonstrate great potential as ultra-stretchable conductors in flexible electronics.

3. Conclusion

Ultra-stretchable SACNT/PDMS conductors are fabricated by stacking parallel or cross-stacked SACNT films onto pre-strained PDMS substrates and forming wavy buckled SACNT structures after the release of the pre-strain. The parallel SACNT/PDMS conductors can be stretched to 200% strain with a normalized resistance increase of only 4.1%. The cross-stacked SACNT/PDMS conductors exhibit even lower resistance variation, with 1.7% resistance change at 40% strain. The parallel SACNT/PDMS conductors exhibit high durability with a resistance increase of less than 5% after 10 000 cycles at 150% strain. *In situ* microscopic observations reveal the formation and straightening of the buckled SACNT structures during the loading and releasing processes with reversible morphology evolution, and the SACNT conductive network can be protected from fracture. The excellent stretchability and resistance stability and high durability of the SACNT/PDMS composite conductors may find broad applications in stretchable interconnections and power devices.

Acknowledgements

This work was supported by the National Basic Research Program of China (2012CB932301), NSFC (51102146 and 51472141), and the NCET Program of China.

Notes and references

1 S. Xu, Y. Zhang, J. Cho, J. Lee, X. Huang, L. Jia, J. A. Fan, Y. Su, J. Su, H. Zhang, H. Cheng, B. Lu, C. Yu, C. Chuang, T.-i. Kim, T. Song, K. Shigeta, S. Kang, C. Dagdeviren, I. Petrov, P. V. Braun, Y. Huang, U. Paik and J. A. Rogers, *Nat. Commun.*, 2013, **4**, 1543.
2 C. Wang, W. Zheng, Z. Yue, C. O. Too and G. G. Wallace, *Adv. Mater.*, 2011, **23**, 3580.
3 T. Yamada, Y. Hayamizu, Y. Yamamoto, Y. Yomogida, A. Izadi-Najafabadi, D. N. Futaba and K. Hata, *Nat. Nanotechnol.*, 2011, **6**, 296.
4 D. Y. Khang, H. Q. Jiang, Y. Huang and J. A. Rogers, *Science*, 2006, **311**, 208.
5 S. p. P. r. Lacour, S. Wagner, Z. Huang and Z. Suo, *Appl. Phys. Lett.*, 2003, **82**, 2404.
6 D.-Y. Khang, J. A. Rogers and H. H. Lee, *Adv. Funct. Mater.*, 2009, **19**, 1526.
7 D. H. Kim, R. Ghaffari, N. Lu and J. A. Rogers, *Annu. Rev. Biomed. Eng.*, 2012, **14**, 113.
8 Z. Chen, W. Ren, L. Gao, B. Liu, S. Pei and H.-M. Cheng, *Nat. Mater.*, 2011, **10**, 424.
9 F. Xu, X. Wang, Y. Zhu and Y. Zhu, *Adv. Funct. Mater.*, 2012, **22**, 1279.
10 M. F. Yu, O. Lourie, M. J. Dyer, K. Moloni, T. F. Kelly and R. S. Ruoff, *Science*, 2000, **287**, 637.
11 T. W. Ebbesen, H. J. Lezec, H. Hiura, J. W. Bennett, H. F. Ghaemi and T. Thio, *Nature*, 1996, **382**, 54.
12 H. J. Dai, *Surf. Sci.*, 2002, **500**, 218.
13 T. Sekitani, Y. Noguchi, K. Hata, T. Fukushima, T. Aida and T. Someya, *Science*, 2008, **321**, 1468.
14 L. Hu, W. Yuan, P. Brochu, G. Gruner and Q. Pei, *Appl. Phys. Lett.*, 2009, **94**, 161108.
15 C. Yu, C. Masarapu, J. Rong, B. Wei and H. Jiang, *Adv. Mater.*, 2009, **21**, 4793.
16 Z. Niu, H. Dong, B. Zhu, J. Li, H. H. Hng, W. Zhou, X. Chen and S. Xie, *Adv. Mater.*, 2013, **25**, 1058.
17 K. L. Jiang, J. P. Wang, Q. Q. Li, L. A. Liu, C. H. Liu and S. S. Fan, *Adv. Mater.*, 2011, **23**, 1154.
18 K. L. Jiang, Q. Q. Li and S. S. Fan, *Nature*, 2002, **419**, 801.
19 X. B. Zhang, K. L. Jiang, C. Teng, P. Liu, L. Zhang, J. Kong, T. H. Zhang, Q. Q. Li and S. S. Fan, *Adv. Mater.*, 2006, **18**, 1505.
20 K. Liu, Y. H. Sun, L. Chen, C. Feng, X. F. Feng, K. L. Jiang, Y. G. Zhao and S. S. Fan, *Nano Lett.*, 2008, **8**, 700.
21 L. Xiao, Z. Chen, C. Feng, L. Liu, Z. Q. Bai, Y. Wang, L. Qian, Y. Y. Zhang, Q. Q. Li, K. L. Jiang and S. S. Fan, *Nano Lett.*, 2008, **8**, 4539.
22 C. Feng, K. Liu, J. S. Wu, L. Liu, J. S. Cheng, Y. Y. Zhang, Y. H. Sun, Q. Q. Li, S. S. Fan and K. L. Jiang, *Adv. Funct. Mater.*, 2010, **20**, 885.
23 Y. Wu, Y. Wei, J. Wang, K. Jiang and S. Fan, *Nano Lett.*, 2013, **13**, 818.
24 X. He, Y. Wu, F. Zhao, J. Wang, K. Jiang and S. Fan, *J. Mater. Chem. A*, 2013, **1**, 11121.
25 S. Luo, H. Wu, Y. Wu, K. Jiang, J. Wang and S. Fan, *J. Power Sources*, 2014, **249**, 463.
26 K. Wang, S. Luo, Y. Wu, X. He, F. Zhao, J. Wang, K. Jiang and S. Fan, *Adv. Funct. Mater.*, 2013, **23**, 846.
27 Y. Wu, H. Wu, S. Luo, K. Wang, F. Zhao, Y. Wei, P. Liu, K. Jiang, J. Wang and S. Fan, *RSC Adv.*, 2014, **4**, 20010.
28 L. Cai, J. Li, P. Luan, H. Dong, D. Zhao, Q. Zhang, X. Zhang, M. Tu, Q. Zeng, W. Zhou and S. Xie, *Adv. Funct. Mater.*, 2012, **22**, 5238.
29 K. Liu, Y. Sun, P. Liu, X. Lin, S. Fan and K. Jiang, *Adv. Funct. Mater.*, 2011, **21**, 2721.
30 K. H. Kim, M. Vural and M. F. Islam, *Adv. Mater.*, 2011, **23**, 2865.
31 M. K. Shin, J. Oh, M. Lima, M. E. Kozlov, S. J. Kim and R. H. Baughman, *Adv. Mater.*, 2010, **22**, 2663.